# Heating samples to 2000 °C and above for scanning tunneling microscopy studies in ultrahigh vacuum ⊕⊘

Buddhika S. A. Gedara <sup>®</sup> ; Michael Trenary **™** <sup>®</sup>



J. Vac. Sci. Technol. B 42, 014201 (2024) https://doi.org/10.1116/6.0003280







Cite as: J. Vac. Sci. Technol. B 42, 014201 (2024); doi: 10.1116/6.0003280 Submitted: 13 November 2023 · Accepted: 18 December 2023 · Published Online: 10 January 2024







Buddhika S. A. Gedara (D) and Michael Trenary (1)

# **AFFILIATIONS**

Department of Chemistry, University of Illinois Chicago, 845 W Taylor St., Chicago, Illinois 60607

a)Author to whom correspondence should be addressed: mtrenary@uic.edu

#### **ABSTRACT**

A simple device for heating single-crystal samples to temperatures ≥2000 °C in ultrahigh vacuum that is compatible with the standard sample plates used in a common commercial scanning tunneling microscope (STM) is described. Heating high melting point samples to higher temperatures than is possible with many existing STM sample holders is necessary to obtain clean, well-ordered surfaces. Results are demonstrated for the (0001) surface of ZrB<sub>2</sub>, which has a melting point of 3050 °C.

Published under an exclusive license by the AVS. https://doi.org/10.1116/6.0003280

## I. INTRODUCTION

Producing atomically clean and well-ordered surfaces of refractory metals and compounds requires heating them to high temperatures in ultrahigh vacuum. This is readily achieved by electron bombardment in which a filament is placed behind the sample that is then biased to a high positive voltage relative to the filament. Once the filament reaches high temperatures, it emits electrons that are accelerated to the sample, heating it to the required temperature. In an early example, King and Wells showed photographs of W(111) and W(110) single crystals mounted in two different ways in front of a W filament. As tungsten has a melting point of 3422 °C, King and Wells found it necessary to heat their crystals to 2000 °C to obtain atomically clean surfaces. They achieved this using 80 W of power with a bias of 600 V. In common with many arrangements for e-beam heating of crystals, their W(111) and W(110) crystals were suspended above the filaments with little contact with the mounting wires so that heat loss by thermal conduction was minimized. A similar arrangement for e-beam heating of crystals for high temperature thermal desorption measurements is described by Yates.3 While such mounting arrangements are ideal for many surface science measurement techniques, it is not compatible with scanning tunneling microscopy (STM). In the widely used commercial STM instruments made by Scienta Omicron, crystals are mounted on plates that are designed

to allow transfer of the samples between the STM and a heating 55 stage. Scienta Omicron offers several high temperature heating is stages such as part numbers PN01720-S, PM05562-S, and CA09051-S, with the highest specified temperature of 2500 K.<sup>4</sup> Here, we describe an electron-bombardment heater that can directly replace the Scienta Omicron heating stage on a standard manipulator that allows samples to be heated up to at least 2000 °C. The electrical connections to the heater use the same electrical feedthroughs and wiring of the standard Scienta Omicron manipulator. Sample transfer from the load-lock region to the heating stage, and from the heating stage to the STM, uses the existing transfer rod and wobble stick. Our design is similar to that of commercial e-beam heaters supplied by Kentax, GmbH and Ferrovac, GmbH, which also allow Scienta Omicron STM sample plates to be heated to at least 2000 °C. However, our heater is designed to directly replace the standard Scienta Omicron heater mounted on a standard Scienta Omicron manipulator. Our design should be of interest to researchers with limited budgets for purchasing commercial high temperature heaters or to researchers interested in making their own customized heaters through modification of our design. Although the performance of our current design is satisfactory, we indicate below at various points where simplifications and improvements could be made. We demonstrate the performance of this design with STM images of the (0001) surface of ZrB<sub>2</sub>, with a melting point of 3050 °C, by showing that a clean

well-ordered surface cannot be obtained with post-Ar<sup>+</sup> sputtering annealing at only 1200 °C, whereas annealing at 1800 °C produces a well-ordered surface with atomically flat (0001) terraces separated by steps one c lattice constant in height.

## II. DESIGN

Critical components of the heater are made from high melting point materials. As the sample plates must reach the highest temperatures, we made these from Ta, which has a melting point of 3017° C. They were sized to exactly replicate the commercial sample plates supplied by Scienta Omicron, which also include ones made from Ta. Due to the difficultly of machining intricate structures out of Ta, other parts, including threaded fasteners, were made from Mo, which has a melting point of 2623 °C.2 Electrical insulators were machined from alumina, which has a melting point of 2045 °C.<sup>2</sup> As shown below, during operation the Mo and alumina components reach much lower temperatures than the Ta plates. We also considered using boron nitride for the electrical insulators as it is easier to machine, but it has less strength at high temperatures. It also has a much higher thermal conductivity than alumina, which is undesirable in this application. Zirconia is also an attractive ceramic and has a lower vapor pressure than alumina at high temperatures,<sup>5</sup> but it undergoes phase changes and an increase in electrical conductivity with temperature, limiting its use to temperatures below 500 °C for many applications.<sup>6</sup> Structural components that do not reach very high temperatures are made of stainless steel.

Figure 1(a) shows the Mo sample plate holder, with a slot for insertion of the Ta sample plate. The slot was machined to exactly

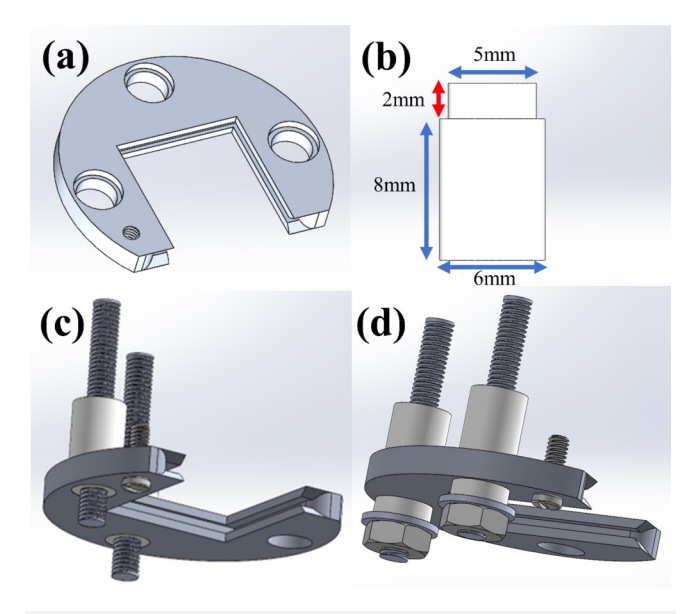


FIG. 1. (a) Sample plate holder. (b) Alumina spacers. (c) Assembly of the sample plate holder, alumina spacers, 2-56 screw, and 4-40 threaded studs. (d) Attachment of the 4-40 threaded studs to the sample plate holder with additional alumina spacers (6 mm outer diameter, 3 mm inner diameter, and 2 mm long), Mo washers and nuts.

match the sample plate thickness for a sliding fit. A fillet was machined at the entrance to the slot to make it easier to insert the sample plate.<sup>14</sup> Although we give most dimensions in millimeters, we also used some available nonmetric fasteners with National Unified Coarse thread designations, specifically 2-56 and 4-40 threaded pieces. Carbide tools were used to machine the Ta and Mo parts, and high-speed steel was used to tap the small hole for a 2-56 screw in this plate. This screw is used to attach a wire to bias the sample plate and holder to high voltage. These parts, therefore, need to be electrically insulated from the filament access plate described below, which is achieved with alumina spacers shown in Fig. 1(b). These pieces were cut from alumina tubing with outer and inner diameters of 6 and 3 mm and were cut to 10 mm lengths with a diamond-edged blade saw. A 2 mm length of the alumina spacers were turned down to an outer diameter of 5 mm using a diamond impregnated grinding wheel. The three counterbored holes were machined in the Mo piece in Fig. 1(a) with 5 mm diameters to a depth of 2 mm with 6 mm diameters for the remaining depth to hold the alumina spacers. Views of the partially assembled sample plate holder are shown in Figs. 1(c) and 1(d). It is held together using Mo 4-40 threaded rod, washers, and nuts (Thermo Shield, LLC). Spacers 2 mm in height were cut from alumina tubing of outer and inner diameters of 6 and 3 mm. These electrically isolate the Mo sample plate holder from the Mo 4-40 threaded rod. Note that although in our original design we intended to assemble the heater using three Mo rods, in practice we found that the heater was sufficiently rigid using only two rods, which is why only two are shown in Fig. 1(d). The design could be revised with plates having only two holes and rods, evenly spaced.

Bottom and top views of the filament access plate are shown in Figs. 2(a) and 2(b). This plate is also made of Mo and is  $\aleph$ machined with slots to accommodate the two alignment pins of the Scienta Omicron transfer rod. These pins must be inserted and 5 held in place so that the transfer rod can be rotated to release the 8 sample plate from the transfer rod pincers. The central groove in this plate is not strictly necessary but was added to provide more space around the filament. The filament access plate is at ground potential during operation. It has counterbored holes 3 and 6 mm in diameter with the latter diameter cut to a depth of 0.5 mm to accommodate the alumina spacers and 4-40 Mo threaded rods. The attachment of the sample plate holder to the filament access plate is shown in Fig. 2(c).

The base plate is shown in Fig. 3. As this plate is expected to reach only moderately high temperatures, it is made of type 316 stainless steel as it has better high temperature properties than type 304, which is generally preferred for most UHV applications because it is the least magnetic stainless steel. It has a small 2-56 tapped hole for attachment of the filament mounting bracket shown in Fig. 4. The hole in the shaft section of the base plate is tapped for a metric M4 screw that allows for attachment to the manipulator via the adapter shown in Fig.  $\mathrm{S1.}^{14}$  The adapter in turn is attached to the manipulator to replace the standard Scienta Omicron sample heating stage. We made the base plate shown in Fig. 3 with tapped holes for 4-40 screws. However, we found it more convenient to use threaded rod with nuts and washers instead. Therefore, nonthreaded through holes in this piece for the 4-40 rods would have been sufficient. Figure 3(c) shows the



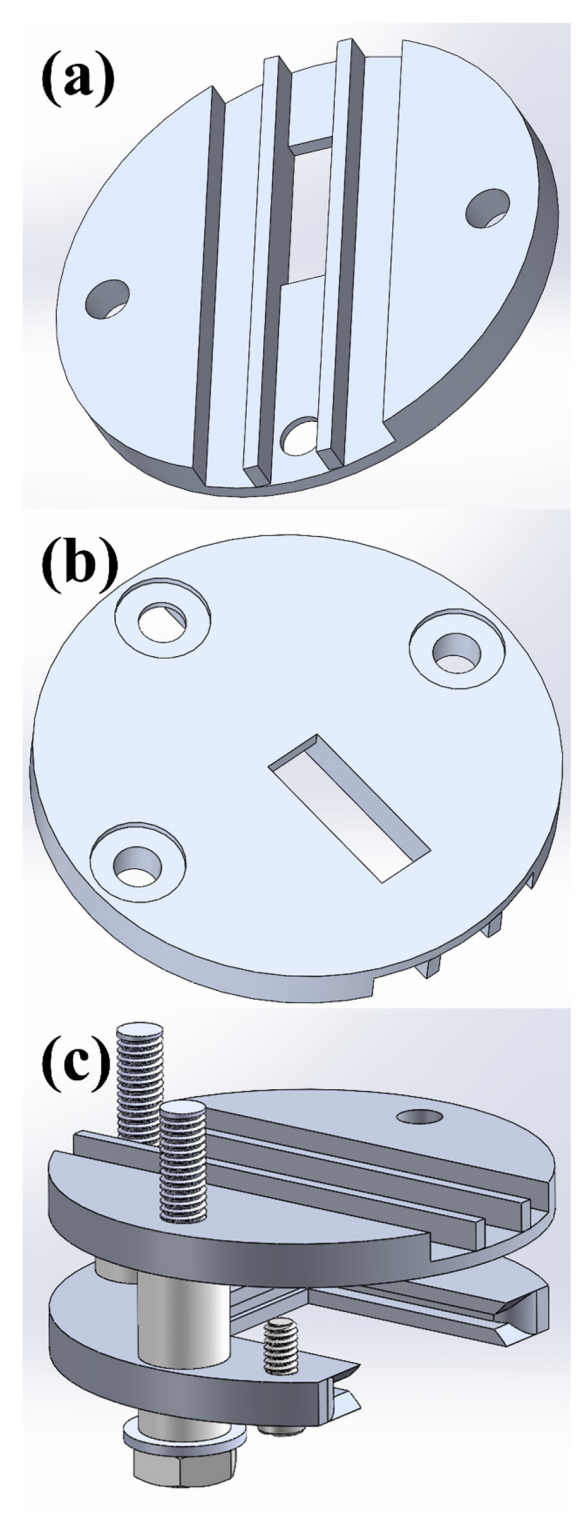
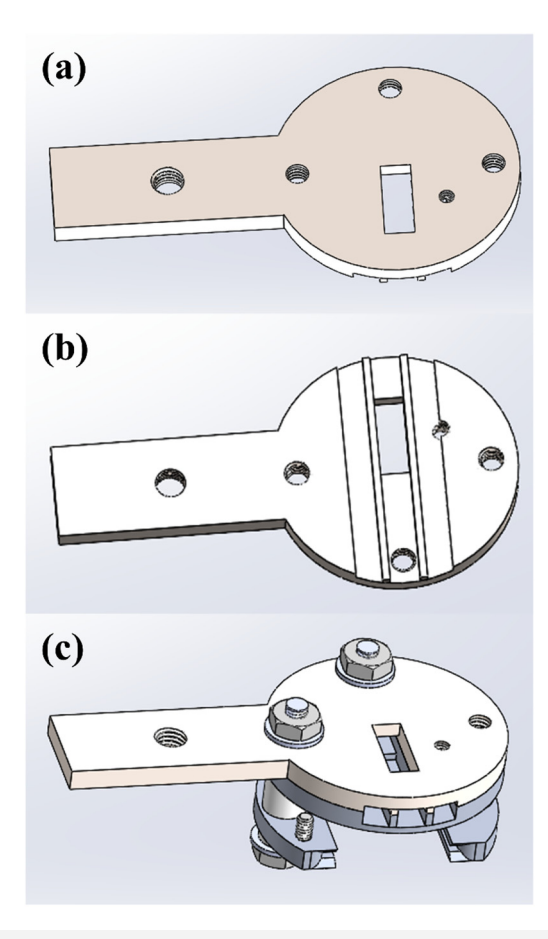


FIG. 2. (a) Top view and (b) bottom view of the Mo plate for access to the filament. (c) Attachment of the access plate to the sample plate holder.

attachment of the base plate to the filament access plate and sample plate holder.

For the electron emitter, we used the filament from a 12 V, 100 W halogen incandescent light bulb (Bi-Pin Base Miniature Light Bulb, Trade Number Q100T4/CL, McMaster Carr). The glass housing of the bulb was cut off with a diamond cutting wheel. As purchased, the filament is rigidly held in a glass base, which avoids the need to devise a filament mount. As incandescent lights are phased out, such conveniently mounted filaments may not be available in the future, in which case it would be necessary to devise a custom-designed filament mount. As the glass filament base has an irregular surface, it is held in place by a thin stainless-steel strap, screwed into the filament mounting bracket. Figure 4(a) shows the disassembled stainless-steel filament mounting bracket with stainless-steel strap, while Fig. 4(b) shows the filament attached to the mounting bracket with the stainless-steel strap. Figure 4(c) shows the filament attached to the assembled heater, and Fig. 4(d) shows a corresponding photograph.

Figure 5 shows the pins from the transfer rod inserted into the slots in the assembled heater. In this view, a sample plate is



**FIG. 3.** (a) Top view and (b) bottom view of the stainless-steel base plate. (c) Attachment of the base plate to the assembly in Fig. 2(c).

partially inserted into the sample plate holder. The pincer has a small pin, not shown, that mates with a small hole in the tab of the sample plate. By rotating the transfer rod, the pincers open to release the sample plate and allow the transfer rod to be withdrawn. The extent of the cutback in the sample plate holder, as shown in the supplementary material, 14 is important; otherwise, the base of the pincer assembly will butt up against the sample plate holder, preventing the sample plate from being fully inserted. Similarly, with the sample plate fully inserted, in trying to remove the sample plate the base of the transfer rod will butt up against the sample plate holder, preventing alignment of the hole in the tab of the sample plate from mating with the pin at the end of the pincer arm.

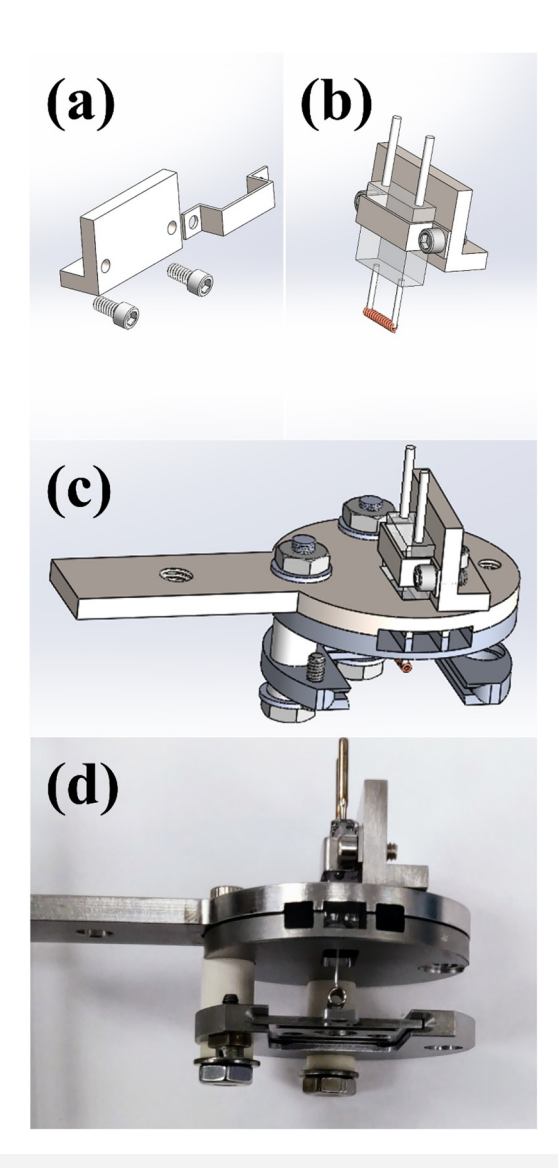


FIG. 4. Filament mounting bracket (a) and assembly (b). Final assembly (c) and photograph (d) of the e-beam heater.

Figure 6 shows photos of two views of the heater attached to the manipulator with the wires connected. The sample plate shown in (a) is a standard plate from Scienta Omicron containing threaded holes and was not used in actual operation. In Fig. 6(b), stainless-steel socket head screws are shown that attached the sample plate holder and filament access plate to the base. However, in initial tests of the heater it was found that the stainless-steel washers between the nut and alumina spacer above the sample plate in Fig. 6(a) melted. These stainless-steel fasteners were, therefore, replaced with Mo threaded rod, nuts, and washers. We also spot welded two Mo foil pieces (see supporting information) to the filament access plates to shield the alumina spacers to prevent deposition of metal evaporated from the filament. The inset in Fig. 6(b) shows the coupler used to connect the posts of the filament to the filament wires.

Figure 7 shows the electrical feedthrough and pins used to supply the filament current and high voltage. It is important for one side of the filament and the high voltage to share the same ground. Although we connected to this feedthrough with the original Scienta Omicron cable and its connector, we opened the other end of the cable for direct connection to the filament and HV supplies. We used several different filament and HV supplies during testing of the heater. For the filament, any power supply (AC or DC) that can provide up to 15 V and 10 A could be used. For the sample bias, a DC power supply that can provide at least +600 V, and up to 300 mA, should be sufficient. Although we used spare power supplies that were already available in our lab, special filament power supplies that regulate the emission current are available, such as from Tectra, GmbH. When not using such a regulated supply, it is important to visually monitor the sample during heating as slight increases in the Cla increases in the filament current and hence temperature can lead to S large unintended increases in emission current. Furthermore, as the sample plate becomes hotter, it can radiatively heat the filament leading to positive feedback and runaway heating of the sample is plate.<sup>3</sup> Such an event occurred when we were using a 600 V, 350 mA power supply, and the emission current suddenly increased to the full value of 350 mA, which melted a Mo sample plate without damage to the rest of the heater. This accident demonstrated that

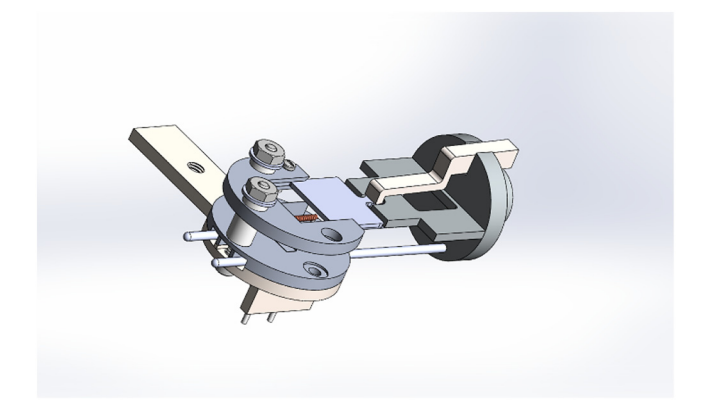


FIG. 5. Insertion of transfer pins into assembled heater.

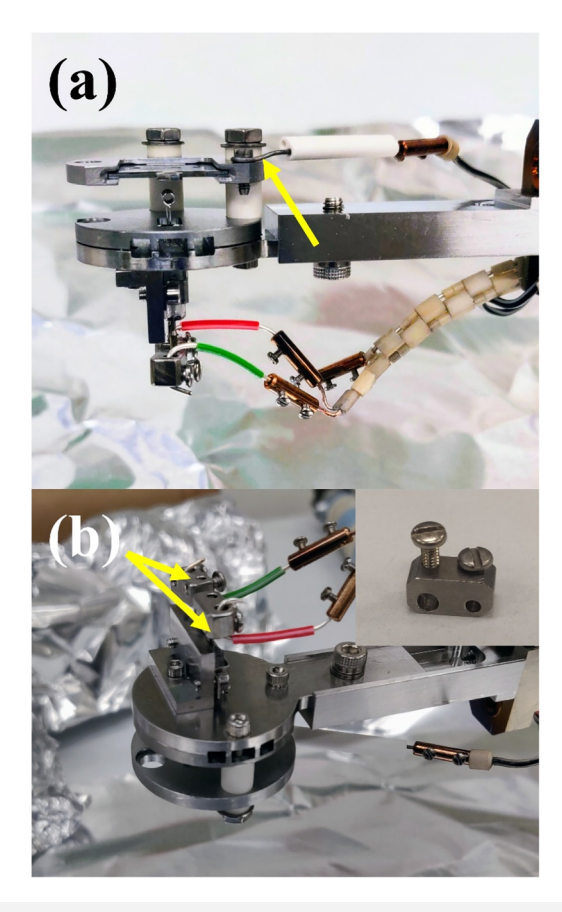


FIG. 6. Photographs of two views of the heater showing the wire connections. In (a), the yellow arrow points to the high voltage connection. In (b), the yellow arrows indicate the connections to the filament leads via couplers one of which

our heater can heat the sample plate to at least the melting point of Mo, 2623 °C. Subsequently, we limited the maximum output current to a value known to be safe.

We did not make use of the thermocouple feedthroughs on the standard manipulator. A thermocouple could be readily attached to the Mo sample plate holder, but as the results below show this remains much cooler than the sample plate, so it would not provide an accurate measurement of the crystal temperature. Measuring the crystal temperature with a thermocouple attached directly to it would require making and breaking electrical contact with thermocouple leads every time the sample is transferred to and from the heater. This is a formidable engineering challenge that we did not attempt to solve. The same limitation applies to the original heating stage where the thermocouple is also not attached to the sample plate, but to a fixed position on the stage near the sample plate. Instead of a thermocouple, we measured sample temperatures with an optical pyrometer. There are two main sources of error in pyrometer temperature measurements. The emissivity, which depends not only on the material, but also on the surface

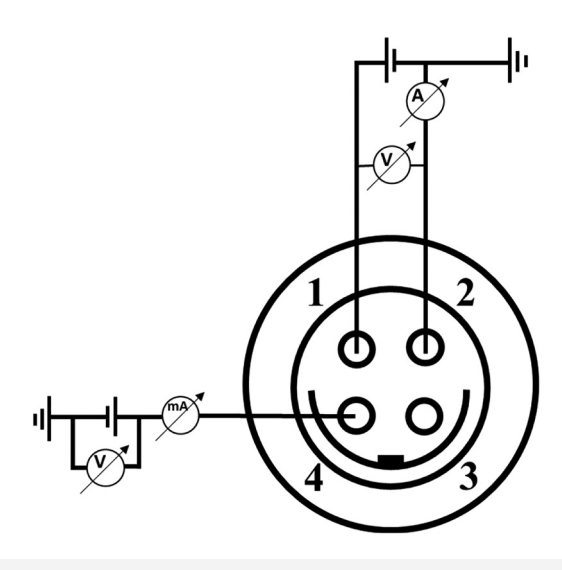


FIG. 7. Electrical connection from the atmospheric side to the Fischer socket of the Scienta Omicron manipulator. Pins 1 and 2 are connected to the Filament+ and Filament-, respectively. Pin 4 is at high voltage (up to +1000 V). These connections are the same as in the original Scienta Omicron configuration except pin 3, which was used for direct heating in the original heater. We connected pin 3 to the base plate, which allowed us to externally ground it.

finish. As our crystals were highly polished to a mirror finish, our reported temperatures are based on an estimated emissivity of 0.15, which is appropriate for polished metals. However, small variations in emissivity in this range can lead to large errors in temperature. 8For example, we measured a ZrB<sub>2</sub>(0001) crystal temperature of  $\frac{4}{8}$ 1888 °C by inputting an emissivity value of 0.1, but changing to an 5 emissivity of 0.2, resulted in a temperature reading of 1390 °C. From this, we conclude that an emissivity uncertainty of ±0.05 could lead to a temperature uncertainty of about ±250 °C. We used two different pyrometers in the measurements, a PYRO Microtherm (Pyrometer Instrument Company) and an OS3708 Portable IR Thermometer (Omega Engineering). Both pyrometers yielded consistent temperature measurements. More advanced pyrometers exist that can minimize error due to uncertainty in emissivity by either simultaneously measuring the emissivity and temperature or by basing temperature measurements on the ratio of energy emission at two-wavelengths, as in the model OS23722 unit from Omega Engineering. One way around the temperature inaccuracy associated with not knowing the exact emissivity would be to temporarily attach a thermocouple to a crystal to establish the value of emissivity needed to bring the thermocouple and pyrometer temperature readings into agreement. After the measuring the emissivity in this way, the thermocouple contact would need to be broken to allow sample transfer. Subsequent pyrometer readings using the established emissivity would then provide more accurate temperature readings. A second source of error is the transmittance of the vacuum chamber window. While a new glass window has a transmittance >95%, chamber windows often become coated by material evaporated from hot filaments and crystals or during dosing of samples with nonvolatile materials. The transmittance of

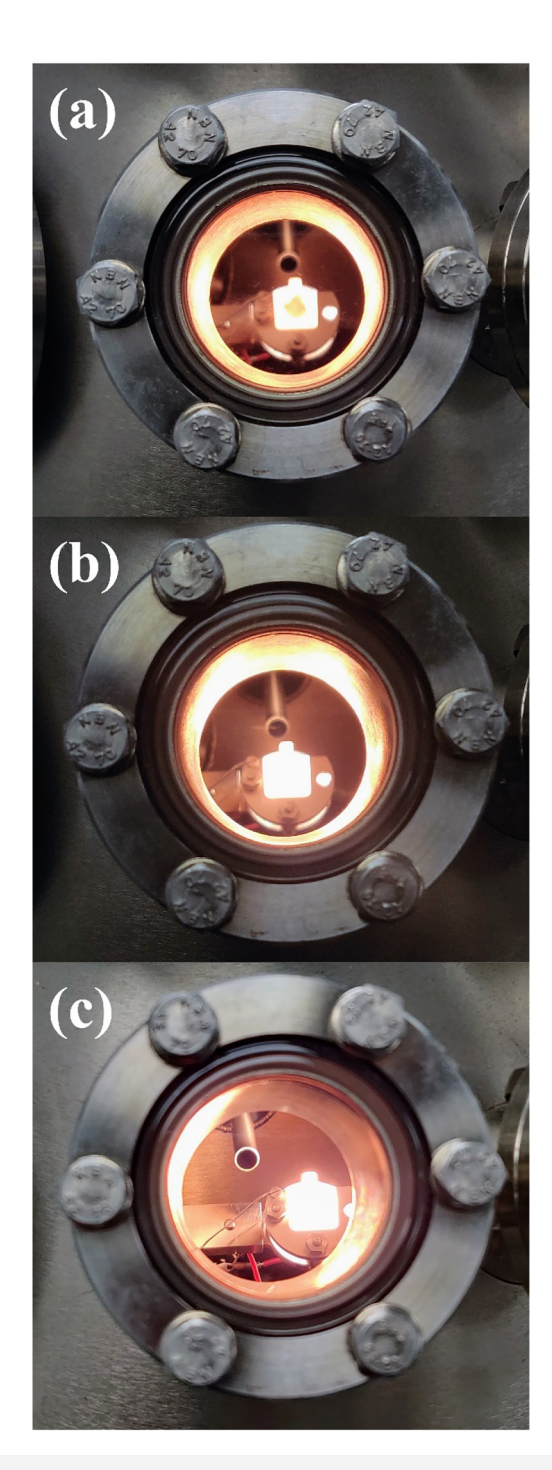


FIG. 8. Photographs of the ZrB<sub>2</sub>(0001) single crystal mounted to a Ta sample plate at different temperatures. The temperature of the crystal was measured with an optical pyrometer using an estimated emissivity of 0.15. In each case, the sample was biased at +600 V. The temperatures, emission currents, filament currents, and filament voltages were (a) ~1200 °C, 100 mA, 6.0 A, 10.2 V; (b) ~1500 °C, 200 mA, 6.4 A, and 10.9 V; and (c) ~1800 °C, 260 mA, 6.6 A and 11.8 V, respectively.

the window will, therefore, decrease with time. A practical method to correct for this problem in using a pyrometer has been described by Yates.<sup>3</sup> Although there is considerable uncertainty in the temperatures reported here, accurate temperature measurements are not essential for the primary purpose of our heater, which is to heat refractory samples to high enough temperatures to obtain clean and well-ordered surfaces as measured with STM.

#### III. OPERATION

The samples are heated by first applying the high voltage with the emission current set to the limit needed to achieve the desired temperature as determined through trial and error. As the filament current is increased, the emission current is read on the HV supply. Measurable emission current was achieved with a filament current of about 5 A. The first time the samples are heated, considerable outgassing occurs, so it takes several rounds of heating to successfully reach higher temperatures, then cooling to allow the chamber pressure to recover. Eventually, it became possible to heat to the target temperatures while the chamber pressure remains in the low 10<sup>-9</sup> Torr range. Because of the high volatility of the oxides of tungsten and molybdenum, this heater is not suitable for annealing samples in the presence of elevated pressures of O<sub>2</sub> or H<sub>2</sub>O.<sup>8</sup> However, as shown below we obtained STM images of the clean Ir (111) surface after annealing at 900 °C in the presence of  $3 \times 10^{-8}$  Torr of O<sub>2</sub>, demonstrating that our heater is compatible with typical surface cleaning procedures in UHV. Figure 8 shows the  $ZrB_2(0001)$  crystal while heating to (a) ~1200, (b) ~1500, and (c) ~1800 °C. Even at 1800 °C, the high intensity of the light <sup>⋈</sup> emitted makes it difficult to distinguish the crystal from the sample plate and a filter is needed to observe the sample. For heating to 1800 °C, we used a power of 156 W (600 V bias, 260 mA emission 28 current). For heating the crystal to 2000 °C, we used a power of 178 W (600 V bias, 297 mA emission current). Figure 9 shows a 🖔 plot of the temperature measured versus the power applied. We used 600 V for the bias voltage simply because that was the maximum voltage available with the power supply used. A higher bias voltage would be desirable as the same power could be

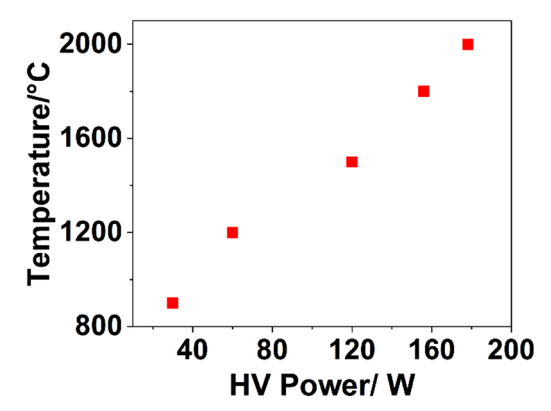


FIG. 9. Plot of the ZrB<sub>2</sub>(0001) surface temperature vs power from the e-beam

achieved with a lower emission current and hence a lower filament current, which would extend the lifetime of the filament. However, we are still using the original filament after heating it hundreds of times. The Mo sample plate holder in Fig. 8 is obviously considerably cooler than the Ta plate, which in turn is hotter than the ZrB<sub>2</sub> crystal. In addition to the ZrB<sub>2</sub> crystal, we have also used the heater with a (111) crystal of Ir, which has melting point of 2446 °C.<sup>2</sup> For the latter, we mounted the crystal over a 2 mm diameter hole in the Ta sample plate, which allowed direct electron bombardment of the crystal, which minimized the difference in temperature between the Ta plate and the crystal. The ZrB<sub>2</sub> crystal was mounted by spotwelding Ta wires over the face of the crystal near its edges to a Ta plate without a hole to avoid large thermal gradients across the crystal. Although borides are extremely hard materials, they are

(a)
60nm
(b)
40nm

**FIG. 10.** STM images of the  $\rm ZrB_2(0001)$  surface after Ar ion sputtering. (a) After annealing to  $\sim$ 1200 °C. Image was recorded at 0.08 nA and 2.0 V. (b) After annealing to  $\sim$ 1800 °C. Image was recorded at 0.30 nA and 1.0 V.

also brittle and are easily cracked in response to heating and cooling.

# **IV. STM RESULTS**

The importance of heating refractory materials such as  $\rm ZrB_2$  to much higher temperatures than possible with the standard Scientia Omicron sample stage is demonstrated by the STM images in Fig. 10. The  $\rm ZrB_2(0001)$  crystal was grown, cut, and polished at the National Institute for Materials Science in Tsukuba, Japan, as described elsewhere. The topographic STM images in Fig. 10 were obtained with a Scienta Omicron variable temperature (VT) STM operated at room temperature. The image in Fig. 10(a) was

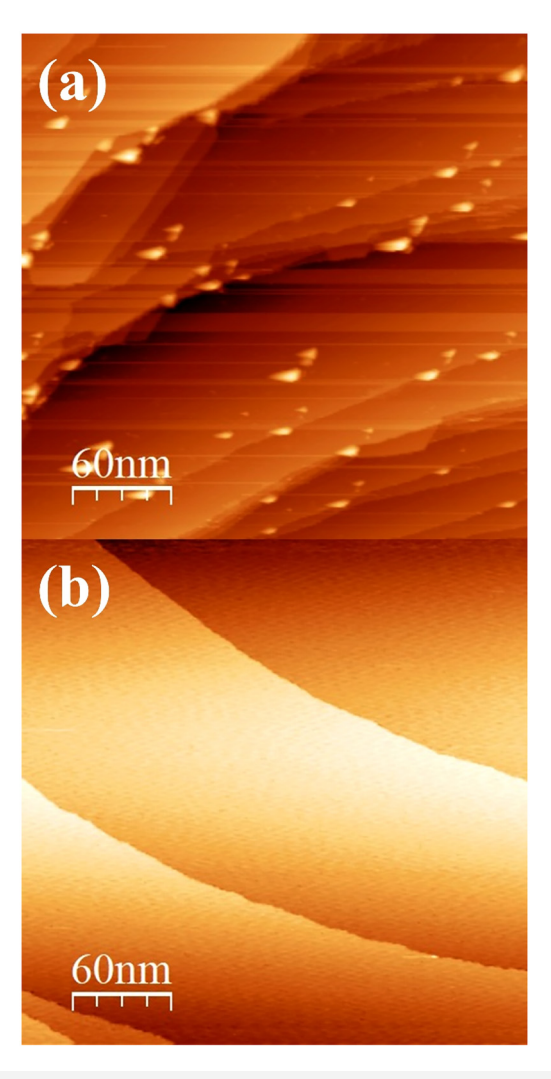


**FIG. 11.** STM images of the Ir(111) surface. (a) After three rounds of Ar+ sputtering and annealing to  $\sim\!1200\,^{\circ}\text{C}$ . Some clusters were observed on the terraces and on the step edges. Image was recorded at 0.2 nA and 2.0 V. (b) After annealing to  $\sim\!900\,^{\circ}\text{C}$  for 10 min in the presence of  $3\times10^{-8}$  Torr of  $O_2$ . Image was recorded at 1.8 nA and 0.8 V.

obtained after argon ion sputtering (1000 V,  $3 \times 10^{-5}$  Torr, for 30 min) followed by annealing for a few minutes at 1200 °C. The image shows vacancy pits, irregular step edges, and considerable contamination. The image in Fig. 10(b) was obtained after additional annealing to 1800 °C and shows smooth featureless terraces separated by steps one c lattice constant (3.52 Å) in height. The generally similar properties of HfB2 and ZrB2 imply that their (0001) surfaces should have similar structures. The images in Fig. 10 are indeed quite similar to what we obtained in an earlier STM study of HfB<sub>2</sub>(0001) using a different commercial STM with a different type of homemade e-beam heater. 12 In the case of HfB<sub>2</sub>(0001), the crystals were annealed to temperatures as high as 2400 °C after sputtering. However, images similar to that of ZrB<sub>2</sub>(0001) were observed following annealing HfB<sub>2</sub>(0001) to 1900 °C. The HfB2(0001) images featured flat Hf-terminated terraces separated by steps 3.4 Å in height, reflecting the slightly smaller c lattice constant of HfB<sub>2</sub>. 13

Figure 11 shows STM images of the Ir(111) surface. The image in Fig. 11(a) was obtained after three rounds of argon ion sputtering followed by annealing to 1200 °C. Small clusters presumably composed of carbon were prevalent on the surface. The image in Fig. 11(b) was obtained after further annealing for 10 min at 900 °C in the presence of  $3 \times 10^{-8}$  Torr of  $O_2$ . This produced a surface featuring flat terraces separated by monatomic steps.

## V. SUMMARY AND CONCLUSIONS

The e-beam heater described here can directly replace the standard heating stage supplied with Scienta Omicron STM systems. We have used it to routinely heat samples up to 2000 °C in a controlled manner and have demonstrated that it can heat sample plates to at least as high as the melting point of Mo. However, we did not test its high temperature limit, and even higher temperatures should be reachable with even higher electron beam powers. There are two major limitations with the current design. First, it does not allow direct measurement of the sample temperature with a thermocouple so that experiments involving heating to temperatures below where pyrometers can be used are difficult. Second, the variable temperature capability of older Scienta Omicron VT-STMs such as ours rely on a double-decker sample holder, which is also incompatible with our design. However, as our e-beam heater simply bolts into the position occupied by the standard sample stage, the two types of stages can be readily interchanged depending on the type of experiment to be performed.

# **ACKNOWLEDGMENTS**

This work was supported by grant from the National Science Foundation (NSF), No. DMR 2119308. We thank Mr. Richard Frueh and Mr. David Kuntzelman of our Physical Sciences Machine Shop for help with the design and fabrication of the heater. We thank Dr. Christian Seidel of Kentax for generously answering technical questions regarding their commercial electron beam heater. We thank Dr. Nathan Guisinger of the Center for Nanoscale Materials at Argonne National Laboratory for helpful discussions about e-beam heating of STM samples and for suggesting the use of the lightbulb filament that we used in our design. We thank Dr. Shigeki Otani for growing, cutting, and polishing the  $\rm ZrB_2(0001)$  crystal used in this study. We thank Dr. Paul Melnikov for technical assistance with the design and operation of the heater.

## **AUTHOR DECLARATIONS**

#### **Conflict of Interest**

The authors have no conflicts to disclose.

#### **Author Contributions**

**Buddhika S. A. Gedara:** Data curation (equal); Investigation (lead); Methodology (lead); Writing – original draft (lead). **Michael Trenary:** Conceptualization (lead); Funding acquisition (lead); Supervision (lead); Writing – review & editing (lead).

## **DATA AVAILABILITY**

The data that support the findings of this study are available from the corresponding author upon reasonable request.

## **REFERENCES**

<sup>1</sup>D. A. King and M. G. Wells, Surf. Sci. 29, 454 (1972).

<sup>2</sup>W. M. Haynes, Editor-in-Chief, CRC Handbook of Chemistry and Physics, 96th ed. (CRC, Coca Raton, FL, 2015).

<sup>3</sup>J. T. Yates, Jr., Experimental Innovations in Surface Science. A Guide to Practical Laboratory Methods and Instruments (Springer-Verlag, New York, 1998).

<sup>4</sup>See https://scientaomicron.com/Services-Support/SpareParts-Catalogues/Spare\_ Parts\_Catalogue\_SO\_Systems\_06\_2019.pdf for *Scienta Omicron* (2023).

<sup>5</sup>See https://www.lesker.com/newweb/deposition\_materials/evaporation-process-notes.cfm for "The Kurt J. Lesker Company" (2023).

<sup>6</sup>See https://www.insaco.com/zirconias/ for INSACO, Inc. (2023).

<sup>7</sup>J. H. Moore, C. C. Davis, and M. A. Coplan, *Building Scientific Apparatus*. *A Practical Guide to Design and Construction*, 2nd ed. (Addison-Wesley Publishing Company, Inc., Reading, MA, 1989).

<sup>8</sup>T. Millner and J. Neugebauer, Nature **163**, 601 (1949).

<sup>9</sup>S. Otani and Y. Ishizawa, J. Crystal Growth 165, 319 (1996).

<sup>10</sup>S. Otani, M. M. Korsukova, and T. Mitsuhashi, J. Crystal Growth 186, 582 (1998).

<sup>11</sup>H. Kinoshita, S. Otani, S. Kamiyama, H. Amano, I. Akasaki, J. Suda, and H. Matsunami, Jpn. J. Appl. Phys. 42, 2260 (2003).

<sup>12</sup>C. L. Perkins, R. Singh, M. Trenary, T. Tanaka, and Y. Paderno, Surf. Sci. 470, 215 (2001).

<sup>13</sup>J. L. Hoard and R. E. Hughes, in *The Chemistry of Boron and Its Compounds*, edited by E. L. Muetterties (Wiley, New York, 1967), p. 26.

14See the supplementary material online for detailed mechanical drawings with dimensions of this and other parts.